MODIS tree cover validation for the circumpolar taiga-tundra transition zone

P.M. Montesano[a], R. Nelson[b], G. Sun[c], H. Margolis[d],
A. Kerber[b], and K.J. Ranson[b]

a. Science Systems and Applications, Inc., Lanham, MD,20706 USA
b. Biospheric Sciences Branch, NASA/Goddard Space Flight Center, Code 614.4, Greenbelt, Maryland, 20771, USA *USA*
c. Department of Geography, University of Maryland, College Park, MD, 20742 USA
d. Centre d'études de la forêt, Université Laval, Québec City, Québec, Canada G1K 7P4

Abstract

A validation of the 2005 500m MODIS vegetation continuous fields (VCF) tree cover product in the circumpolar taiga-tundra ecotone was performed using high resolution Quickbird imagery. Assessing the VCF's performance near the northern limits of the boreal forest can help quantify the accuracy of the product within this vegetation transition area. The circumpolar region was divided into 7 longitudinal zones and validation sites were selected in areas of varying tree cover where Quickbird imagery is available in Google Earth. Each site was linked to the corresponding VCF pixel and overlaid with a regular dot grid within the VCF pixel's boundary to estimate percent tree crown cover in the area. Percent tree crown cover was estimated using Quickbird imagery for 396 sites throughout the circumpolar region and related to the VCF's estimates of canopy cover for 2000-2005. Regression results of VCF inter-annual comparisons (2000-2005) and VCF-Quickbird image-interpreted estimates indicate that: (1) Pixel-level, inter-annual comparisons of VCF estimates of percent canopy cover were linearly related (mean $R^2 = 0.77$) and exhibited an average root mean square error (RMSE) of 10.1% and an average root mean square difference (RMSD) of 7.3%. (2) A comparison of image-interpreted percent tree crown cover estimates based on dot counts on Quickbird color images by two different interpreters were more variable ($R^2 = 0.73$, RMSE = 14.8%,

RMSD = 18.7%) than VCF inter-annual comparisons. (3) Across the circumpolar boreal region, 2005 VCF-Quickbird comparisons were linearly related, with an R^2 = 0.57, a RMSE = 13.4% and a RMSD = 21.3%, with a tendency to over-estimate areas of low percent tree cover and anomalous VCF results in Scandinavia. The relationship of the VCF estimates and ground reference indicate to potential users that the VCF's tree cover values for individual pixels, particularly those below 20% tree cover, may not be precise enough to monitor 500m pixel-level tree cover in the taiga-tundra transition zone.

MODIS; validation; tree cover; ecotone; transition; taiga; tundra; circumpolar

Introduction

Over the next century, estimates of global temperature increases range from 1.8° C to 4.0° C, but this warming will not be distributed evenly around the globe (IPCC 2007). The Arctic regions are expected to warm approximately twice as fast, 4° C to 7° C by 2100, and much of that warming may occur in the autumn and winter months (Serreze & Francis 2006; Hassol 2004). Large changes in high-latitude forest structure and extent are possible and, in fact, have already been documented. For example, in the 1980s and 1990s between 40° N and 70° N, increases in photosynthetic activity have been linked to changing spring land surface temperatures (Goetz et al. 2005; Zhou et al. 2003; Randerson et al. 1999; Myneni et al. 1997). There is modeled, remotely-sensed, and field-measured evidence of changes in fire regime, insect infestations, treeline migration, age class structure and species distribution in northern forests (Soja et al. 2007, Kurz et al. 2007, 2008a,b). Trees may respond to a warming environment by moving northward and upslope, however, southward treeline movements are possible as permafrost melts,

55 soils saturate, and bogs and wetlands replace forests (Crawford et al. 2003; Schuur et al.
56 2008). As the northern boundaries of the circumpolar boreal forests become less certain,
57 there is a need to develop remote sensing techniques to monitor changes in the transition
58 zone between the taiga and tundra, forest extent and treeline location as forests respond to
59 the changing climate and disturbance regimes (Frey et al. 2007). The taiga-tundra
60 transition zone is the largest ecotone on earth, stretching over 13,400 km.

61 The MODIS sensor, part of NASA's Earth Observation System (EOS) onboard
62 the Terra and Aqua satellites, is designed for moderate-resolution global monitoring of
63 the Earth. The Vegetation Continuous Fields (VCF) product is derived from multiple
64 temporal composites and provides a percent canopy cover value for each 500m pixel.
65 This continuous value (0-100%) is related to the amount of skylight obstructed by tree
66 canopies equal to or greater than 5 meters in height. This percent canopy cover term
67 differs from percent tree crown cover (TCC) measured for the Quickbird imagery (see
68 below), where the latter refers to the sum of the canopy cover and the within-crown
69 skylight (Hansen et al. 2003). This continuous value approach to land cover mapping can
70 be used along with more conventional land cover categorical data to more reliably map
71 global land covers. The heterogeneous nature of land cover at ecotone boundaries lends
72 itself to the continuous mapping method of the VCF and there have been other efforts to
73 map tree cover in this manner around the world (Cross et al. 1991; Zhu and Evans 1994;
74 Mayaux and Lambin 1997; Tottrup 2007; Heiskanen and Kivinen 2008).

75 We validated the accuracy of this product within the taiga-tundra transition zone
76 using validation sites distributed throughout the circumpolar boreal and taiga-tundra
77 transition zone. We addressed how VCF pixels compare inter-annually and the
78 differences in TCC interpretations from high-resolution optical Quickbird satellite

79 imagery between different interpreters to assess the variation that is inherent in human
80 estimation of TCC from high-resolution imagery. Finally, we examined comparisons of
81 VCF pixels and visual interpretations from Quickbird imagery.
82
83 **Background**
84 The changing abundance of trees along the taiga-tundra transition zone has been
85 used to monitor shifts in vegetation patterns that may signal a response to human
86 activities and/or climatic changes. Treeline changes occur where temperature changes
87 are most profound and a possible circumpolar trend has been suggested (Esper and
88 Schweingruber 2004). Satellite observations have shown that northern latitudes (Zhou et
89 al. 2003), and specifically the boreal forests (Bunn and Goetz 2006), respond in different
90 ways to changing climate. Because of the variability related to the response of the boreal
91 treeline to climate change, there is a critical need for accurate mapping of land cover and
92 monitoring of changes with consistent monitoring methods (Frey et al. 2007; Esper and
93 Schweingruber 2004). Sun et al. (2004) used a spectral un-mixing method with Landsat
94 data to characterize the transition from taiga to tundra for a forest island in northern
95 Russia. Heiskanen and Kivinen (2008) concluded that the use of multi-angular and –
96 temporal data can increase the accuracy of 1km resolution tree cover estimates of the
97 peak growing season in the taiga-tundra ecotone in northern Scandinavia.
98 With a nominal 500m spatial resolution, the VCF product incorporates multi-
99 spectral and -temporal data, capturing phenological differences, to estimate the
100 proportion of canopy cover in each pixel. The VCF resolution may also be suitable for
101 studying ecotone dynamics (Stow et al. 2004). This technique allows for heterogeneous
102 areas to be better represented than is possible by discrete land cover classes.

Heterogeneous areas, such as the taiga-tundra transition zone, lend themselves to this type of depiction because groups of percent cover pixels can represent gradients across space. The product is derived from a regression tree that interprets the biophysical relationship between the satellite spectral signals and vegetation cover throughout a season and a linear regression model that helps improve the regression tree's predicted values (Hansen et al. 2002b). The VCF algorithm is kept constant for each year's data, so robust MODIS data processing is a key factor in the year-to-year consistency of the VCF. Furthermore, this method of statistically estimating sub-pixel tree cover at global scales is necessary because individual trees cannot be resolved by the sensors required for regional and global level satellite monitoring (Rees et al. 2002).

MODIS data products have been validated at a sub-regional scale by using previously collected field data or higher resolution image data extending across the study area (Pisek and Chen 2007; White et al. 2005; Hansen et al. 2002a; Hansen et al. 2003). White et al. (2005) used 3954 plots from two independent datasets to test the VCF correlation with ground measurements of tree cover in the southwestern United States. They found an overall negative bias, whereby VCF underestimated tree cover (31% and 24% overall for the two datasets) and the RMSE generally increased with increasing tree cover. The authors advised using the Version 1 VCF with caution in this part of the world. However, as this version has been superseded with subsequent versions, with consequent changes to the algorithm, the relationship of ground data to VCF values for this area should be reassessed using the most currect product. Hansen et al. (2002a) performed a validation of an early VCF version in Zambia using high resolution IKONOS and Landsat data. After classifying the higher resolution imagery and scaling up to MODIS resolutions, the RMSE was 5.2%. The two different levels of validation

127 success revealed by these studies indicate that the VCF's ability to reliably estimate
128 percent canopy cover may vary greatly depending on factors such as ecoregion and
129 latitude. In northern Finland, Heiskanen (2008) compared the VCF with other global
130 scale map products, finding that the VCF overestimates values in low tree cover and
131 underestimates values in high tree cover. The author also noted the difficulty in mapping
132 tree cover in the taiga-tundra transition zone and the difficulty of obtaining field data.
133 There have also been validations of MODIS land products at the pixel level. Liu
134 and Mishchenko (2008) compared measurements of aerosol optical thickness from
135 MODIS and MISR for collocated pixels. Morisette et al. (2003) discussed the use of
136 IKONOS and Landsat ETM+ for exploring variation within a MODIS pixel.
137 Salomonson et al. (2006) compared percent snow cover within individual MODIS 500m
138 pixels to the percentage of Landsat ETM+ derived snow cover for corresponding grid
139 cells. Hall et al. (2008) examined MODIS level 2 land surface temperature (LST) pixels
140 in the sinusoidal grid with LST values derived from Landsat ETM+ and ASTER of the
141 same area. The LST values from MODIS pixels were also compared with automatic
142 weather station data at high latitudes (Greenland). The authors found that single weather
143 station point observations of temperature could not be reliably compared with 1km
144 MODIS, 90m ASTER, or 57m ETM+ pixels because the point measurements don't
145 represent the variation of temperature across the area covered by each pixel. The authors
146 suggested that a local array over areas corresponding to pixels used in the comparison
147 would appropriately characterize the internal heterogeneity of surface temperature within
148 a pixel. The latter two studies used regression to relate the MODIS product values in
149 high latitudes to the ground reference data at the pixel level.

In place of on-site validation, some studies have acquired ground reference from high-resolution imagery displayed in Google Earth (GE). Using the Quickbird imagery in GE, measurements have been made of river channels and oxbow lakes (Constantine and Dunne 2008) as well as irrigated areas (Thenkabail et al. 2008). Luedeling and Buerkert (2008) visually interpreted GE's high-resolution data in areas randomly distributed across a study area to validate a Landsat-based classification of desert oases in Oman. In this study, we use GE's archive of Quickbird imagery to validate the MODIS VCF product for northern boreal forests. These Quickbird images in GE cannot be spectrally enhanced nor can band combinations be reconfigured. The imagery is displayed in true-color and the near infrared channel cannot be accessed, which reduces the information content available to image interpreters. There is, however, some basic image information metadata accessible through the "DigitalGlobe Coverage" sub-layer under the pre-packaged "More" layer contained in the GE "Primary Database." Activating this information reveals an icon at the center point of each Quickbird image that links to a web thumbnail version of the image along with the Catalog ID number, acquisition date, latitude and longitude of the image center, off nadir angle, target azimuth, cloud cover, and environmental quality.

Methods

Identifying validation sites in Google Earth

We selected sites throughout the circumpolar boreal forest that included a range of percent TCC for which there was high resolution, true-color Quickbird imagery available in GE. Only images with resolutions that allowed interpreters to identify individual tree crowns were considered in the selection process and the majority of

174 images were acquired from May-September. To ensure that our sites were well
175 distributed throughout the circumpolar northern boreal region, we divided Eurasia above
176 60° N into 4 regions and North America above 55° N into 3 regions and selected
177 approximately 60 validation sites for each of these seven zones (Figure 1). The
178 validation sites extended southward to 55 ° N in North America to include the taiga-
179 tundra transition zone of eastern Canada, where biophysical characteristics in this region
180 begin to limit tree growth at this latitude. The southern limits of study sites in both
181 Eurasia and North America were chosen based on information from various
182 interpretations of treeline, ensuring that these limits allowed us to consider tree cover
183 within the transition zone from boreal forest to tundra (Timoney et al. 1992, Callaghan et
184 al. 2002a, Olsen et al. 2001). The seven circumpolar regions include: Scandinavia,
185 Western Eurasia, Central Eurasia, Eastern Eurasia, Alaska, Central/Western Canada, and
186 Eastern Canada. In each zone, at least 20 test sites were identified in the boreal forest in
187 each of three TCC categories: 0-20%, 20-60%, 60-100%. In a given region, we selected
188 every point based on (1) the availability of high-resolution (2.44m at nadir) Quickbird
189 imagery in GE, (2) our initial, quick-look, visual assessment/estimate of percent TCC
190 category (i.e., 0-20%, etc), and (3) on landscape/forest homogeneity surrounding the
191 location (approximates a 3x3 MODIS 500m pixel window size). This third criterion was
192 introduced to try to mitigate mis-registration errors between the GE imagery and the
193 MODIS VCF pixels. The percent canopy cover values of the corresponding local VCF
194 pixels were not considered during this site selection process.
195 Sites were located at least 15 km apart to spread the VCF evaluation pixels across
196 a given zone and to introduce spatial independence into the site selection process. We

197 selected 431 sites (7 zones x 3 TCC classes x 20 locations + 11 additional unique/unusual
198 sites).
199
200 *MODIS VCF Mosaics*
201 We obtained the latest VCF data, downloaded by MODIS tile, through the
202 University of Maryland's Global Land Cover Facility
203 (ftp://ftp.glcf.umiacs.umd.edu/modis/VCF). The Collection 4 version of the data used for
204 this validation was collected for MODIS tile rows 2 and 3. Tile row 1 (above 70° N) was
205 not available at the time of the analysis. Tile mosaics in the native sinusoidal projection
206 for North America and Eurasia were created using the MODIS Reprojection Tool version
207 4.0 from the Land Processes Distributed Active Archive Center (http://lpdaac.usgs.gov).
208 Horizontal tiles 9-14 were used for North America and tiles 18-26 for Eurasia (Figure 2).
209 While each MODIS pixel is nominally 500m X 500m, they are in fact 463m on either
210 side in the original sinusoidal projection. This detail is important for generating precise
211 TCC sampling grids.
212
213 *Matching validation sites, VCF pixels and Google Earth imagery*
214 The comparison of percent TCC estimates from Quickbird imagery in GE to
215 MODIS VCF pixel values of percent canopy cover requires accurately matching the VCF
216 pixels with their corresponding spatial locations in GE to the extent possible given
217 MODIS geo-location error limits. The VCF pixel whose centroid was closest to each
218 location selected in GE was identified and the boundary of each pixel, geo-located
219 according to the four corners, was overlaid on the GE imagery. We then generated
220 regular 10 X 10 dot grids for each VCF pixel such that each dot represented the center of
221 an area that was one-tenth the length and width of the VCF pixel. The boundaries of the

222 selected pixels for each of the 7 circumpolar zones along with the regular dot grids were
223 then converted to Keyhole Markup Language (KML) files and displayed in GE. Since
224 the MODIS data was in its native sinusoidal (equal area) projection with an accuracy of
225 50m (1σ) (Wolfe et al. 2002), the VCF pixel boundaries displayed in GE and associated
226 dot grids did not maintain the square shape of a gridded cell, but preserved the areal
227 coverage, location and extent that the pixel represented (see Figure 3). We note that the
228 sinusoidal projection does not increase inaccuracy beyond the geo-location accuracy
229 stated above.
230
231 *Estimating percent tree cover*
232 Five interpreters systematically viewed a subset of the validation sites, counting
233 the number of dots that lay atop tree crowns. Prior to the image interpretation,
234 interpreters collectively reviewed test sites composed of a range of TCC densities and
235 types at various latitudes and various regions in order to standardize interpretations of
236 tree cover. The interpreters counted dots, for each assigned VCF pixel, lying atop tree
237 crowns to provide an estimate of percent TCC. The following guidelines were used to
238 determine if a dot lay atop a tree crown:
239 1. The entire dot must intercept a tree crown. As each dot represents an
240 infinitesimally small point on the earth, i.e. it has no area, increasing the
241 scale (zooming in) reveals the placement of the dot in relation to tree
242 crown pixels. Note: Increasing the scale will not alone determine whether
243 a dot intercepts a tree crown, because the context of surrounding pixels is
244 needed to identify features.

2. The feature beneath a dot had to be distinguished from shrubs. The two central indications of tree crown presence were:
    a. the shape of the crown, and
    b. the presence of a shadow.

In cases of continuous dense tree cover, where shadows and shape did not help identify individual trees, the broader spatial context and texture of the forest patch and local landscape patterns helped to determine whether a dot intercepted a tree crown or a shrub.

The VCF product measures percent canopy cover, where canopy cover is defined as the component of TCC that obstructs skylight (Hansen et al. 2003). Percent TCC was interpreted, rather than percent canopy cover, because our validation approach relied on Quickbird imagery where canopy cover and within-crown gaps could not be distinguished. From an interpreter's perspective, TCC is the metric that can be visually estimated.

Each site was attributed a value based on an interpreter's count/estimate of tree/no tree for each of the 100 dots regularly arranged within a VCF pixel's boundary. Each site's value was then associated with the corresponding values of VCF pixels for years 2000-2005. This data set allowed us to examine the consistency of the VCF from one year to the next. Furthermore, 58 of the 396 sites were systematically selected for replicate image-interpretations by two of the five image-interpreters. This re-examination of 15% of the sample allowed us to investigate the variability among the five image interpreters. Interpretations of percent TCC were made for 424 of the 431 sites because seven sites were judged, after examining the imagery, to be too difficult to confidently discern trees from shrubs, i.e., the images were either too dark or too blurry

to permit accurate estimation of TCC. Quickbird – VCF regressions were based on 396 sites since there were no Collection 4 VCF values for 28 sites above 70° N. Sites for which multiple interpretations of tree cover differed by more than 30 percentage points were examined to investigate and resolve the differences in the tree cover estimates. In these instances, the interpreters involved discussed the scene, and interpretations were redone to better standardize image-interpreted estimates. A reduced major axis (RMA) regression was used to compare a later VCF year's data with an earlier year's, and one interpreter's TCC estimates to another's. The RMA regression is appropriate for comparing 2 year's of VCF data and 2 interpreter's estimates of TCC because there are similar amounts of error in data on both axis, i.e., in both X and Y (Curran and Hay 1986).

Results

Inter-Annual Comparisons

Figure 4 reports the slopes of the simple linear regression lines relating Quickbird estimates to VCF estimates for each zone for 2000-2005. While there are differences between longitudinal zones, most slopes (64%) are between 0.4 and 0.6 and all slopes for all zones were less than 1 reflecting the varying relationship of Quickbird image-interpreted estimates and VCF values at the low and high ends of the canopy cover range. This relationship is examined in subsequent figures. Results for Scandinavia report regressions with low slope values throughout the study time period. Visual examination of the data in this region reveals what may be some systematic processing bias in that VCF canopy cover values show an abrupt change in northern Scandinavia that are not indicative of natural patterns or land use.

293 We compared the VCF canopy cover values with the Quickbird TCC
294 interpretations at the 396 validation sites. Figure 5 shows the distribution of each
295 Collection 4 VCF dataset from 2000-2005 with the validation site estimates using an
296 amalgam of cloud-free data (2002-2008) from the Quickbird satellite. This provides
297 information on the variability of the VCF from 2000-2005, as the appearance of each
298 frequency distribution plot helps to explain the consistency of the VCF and where there
299 may be systematic differences from ground-truth validation. To generate Figure 5, each
300 of the yearly VCF estimates and the image-interpreted estimates of percent TCC were
301 assigned to a 10% bin (e.g., 0-10%, 11-20%,... 91-100%) and a count made. The
302 majority of VCF pixels at the 396 sites report canopy cover values between 20 and 60%.
303 While the difference between iterations of the VCF is minimal in this range, they are
304 distinctly higher than the image-interpreted estimates of percent TCC. A Kolmogorov-
305 Smirnov Test for two independent samples was performed to compare the distributions of
306 the earliest and latest (2000 and 2005) VCF data and confirmed that the differences in
307 these yearly VCF distributions are in fact not significantly different ($p = 0.939$). The
308 distributions of the image-interpreted estimates and the 2005 VCF data were tested in the
309 same manner, confirming a significant statistical difference ($p < 0.001$). The frequency
310 distributions of each yearly VCF estimate suggest that the VCF tends to underestimate
311 canopy cover in areas where Quickbird reports TCC < 20% and overestimates in areas
312 where Quickbird reports TCC > 20%. In addition, this figure shows that there are no
313 VCF values above 80% canopy cover (discussed in a subsequent section).

314 We also examined VCF inter-annual variability with regression in order to
315 characterize the precision of the VCF product. Figure 6 shows the inter-annual variation
316 on a pixel-by-pixel basis for 403 circumpolar ground sites for each combination of VCF

317 years (2000-2005). This set of regressions explains the relationship of all VCF estimates
318 available to date for 403 sites. In interpreting the regressions in Figure 6, we assume that
319 from 2000-2005 actual canopy cover changes little at the each site, though certainly
320 forest disturbances, such as fire, could alter the canopy cover in this time period. Simple
321 t-tests indicate that most slopes are not significantly different from 1.0 and most
322 intercepts are not significantly different from zero (Table 1). At the pixel level, the inter-
323 annual scatter, 2004 to 2005, amounted to RMSE < 10% and RMSD = 7%, though the
324 greatest range discrepancy across all sites was 38% (61% in 2005 with 23% in 2004 and
325 47% in 2005 with 9% in 2004). The inter-annual scatter for all combinations of years
326 ranged from a RMSE = 9.5 to 10.8% and a RMSD = 6.8 to 7.8%.
327
328 *Variability of Quickbird TCC Interpretations*
329 Figure 7 presents the variation inherent among Quickbird image interpreters.
330 Different pairs of interpreters estimated %TCC on 58 of the 396 validation sites to
331 quantify the variability associated with our image-interpreted tree counts. The VCF
332 product (Figure 6) is less variable, i.e., more stable (average RMSE = 10.1%, average
333 RMSD = 7.3%) than the Quickbird image-interpreted estimates (RMSE = 14.8%, RMSD
334 = 18.7%) which serve as our ground reference data product. There were 15 estimates for
335 which at least a 30 percentage point difference in tree cover interpretation occurred. The
336 majority (12) of these involved shrub/tree confusion by one of the interpreters. These
337 estimates were re-done after interpreters re-calibrated their understanding of tree cover
338 appearance for these sites, to further standardize ground reference.
339
340 *Percent Tree Crown Cover by Circumpolar Zone*

341 Using the most recent (2005) version of the Collection 4 VCF, we correlated the
342 observed Quickbird percent TCC values with the percent canopy cover estimates of the
343 VCF for each of the 7 zones and for all zones combined (Figure 8). Table 2 summarizes
344 the simple linear regression results for each of the plots in Figure 8. Each zone had a
345 minimum of 45 validation sites. The scatter varies for each zone, with no apparent bias
346 towards any percent TCC interval. Some of the more inconsistent data points were
347 investigated and found in some cases to be at the boundary of an abrupt change in VCF
348 percent canopy cover or in an area where shrub cover had a tone and texture similar to
349 that of nearby stands of trees. Tests confirmed that all slopes were different than 1 and
350 all Y-intercepts were different than 0 (Table 2). The Scandinavian sites had a slope that
351 was significantly different than the slope for all zones combined ($p < 0.001$).
352 We note the following in Table 2 and Figure 8: (1) an upper VCF bound of 80%
353 in all graphs in Figure 8 (also apparent in Figure 6), (2) a consistently positive y-intercept
354 significantly different from zero in all zones, and (3) RMSE values ranging from ~10-
355 15% and RMSD values ranging from ~ 14–23% (with the exception of Scandinavia).
356 The 80% upper VCF limit noted in Figures 6 and 8 in both North America and Eurasia is
357 consistent with other reports on the VCF product (White et al. 2005; Mark Carroll,
358 personal communication). Hansen et al. (2003) explains that this 80% upper VCF limit is
359 due to the relationship between TCC and canopy cover. On average, 80% canopy cover
360 corresponds to complete crown cover. However, we might expect the canopy cover to
361 TCC ratio to vary depending on the different crown cover densities of the dominant tree
362 types across regions.
363 For low percent TCC values, the y-intercepts show a range from about 11% to
364 nearly 25%, indicating the VCF's tendency to overestimate crown cover in areas that are

365 more lightly forested. The consistent, positive y-intercepts may indicate some tendency
366 of the VCF to confuse tall shrubs as trees. Certainly the Quickbird image interpreters had
367 this same problem, and a considerable amount of time was spent by the interpreters trying
368 to discern and define the difference between shrubs and trees in some of the imagery.
369 However, where the 2005 VCF values were less than 20% canopy cover (49 sites), 73%
370 of the Quickbird estimates were also less than 20 (36 sites) and only 7 of the remaining
371 13 fell outside the RMSE range (14%). This indicates that while the VCF may err in
372 areas where trees are scarce and shrubs are abundant, the Quickbird estimates tend to
373 confirm the VCF low percent canopy cover values.

374 The entire circumpolar region had an overall RMSE and RMSD of 13.4% and
375 21.3%, respectively. We view the zonal and circumpolar RMSE and RMSD values
376 reported in Table 2 and Figure 8 as worst-case estimates given that some unknown
377 portion of this error term is due to variation associated with the image-interpretation
378 results. This 13.4% RMSE is lower than the values reported by White et al. (2005) for
379 the southwestern United States (24% and 31%) and higher than the values reported in
380 Hansen et al. (2002a) for Zambia (5.2%).

381

382 **Limitations and Uncertainties**

383

384 It is helpful to understand the spatial and temporal context in which our ground
385 reference was gathered and the VCF produced. Limitations to, and uncertainties in,
386 accurately assessing tree cover at a given location may stem from the method of
387 collecting ground reference, satellite data geo-location/gridding, and the timing of
388 satellite data for compiling both the ground reference and the VCF data product.

389 The variability in Figure 7 indicates the ease with which similar estimates will be
390 repeated and the inherent difficulty of remote satellite and visual estimation of percent
391 canopy cover and TCC. Although standardization protocols were established prior to the
392 validation effort, there were a number of cases in which the five interpreters differed in
393 their interpretation of tree cover. The replicated site interpretations of percent TCC were
394 done by five interpreters, which likely increased the level of disagreement between site
395 interpretations than if sites had been re-interpreted by the same interpreter. Thus, the
396 overall uncertainty in ground reference is not surprising. The similar image tone and
397 texture of trees and shrubs combine with different interpretations of these features by five
398 interpreters to create noisy validation data. The purpose of re-examining those replicated
399 sites that differed by at least 30 points was to minimize differences based on strong
400 interpreter bias where an errant interpretation of tree cover could dramatically effect
401 overall interpreter precision. A lower threshold would have allowed for examination of
402 smaller discrepancies and refinement of a greater number of the replicated estimates,
403 resulting in a higher level of consistency.

404 We chose this conservative threshold so as not to disguise the true noisy nature of
405 the ground reference. The level of variability in the ground reference makes it difficult to
406 pinpoint the extent to which the VCF estimates of low canopy cover, in the transition
407 zone and throughout the boreal forest, vary from true tree cover. However, the overall
408 RMSE and RMSD (13.4% and 21.3% respectively) are evidence that below 20% VCF
409 canopy cover the ability of the product to provide reliable 500m pixel-level delineation of
410 the circumpolar taiga-tundra transition zone is limited.

411 The accuracy of the MODIS VCF product may also introduce discrepancies
412 between VCF percent canopy cover values and interpreted percent TCC. MODIS' sub-

413 pixel geo-location accuracy (at nadir) may contribute some positional inaccuracies, as
414 will Quickbird's geo-location accuracy (+/- 23m, CE90%), and we also note that the
415 gridding of some observations could also contribute to disagreement between
416 interpretations of percent TCC and VCF values. Heiskanen and Kivenen (2008) indicate
417 that per-pixel comparison of reference data with gridded MODIS Level 1B data is
418 complicated by the fact that some gridded values represent different areas on the ground
419 than do the original satellite observations from which the gridded values were derived.
420 This is due to the MODIS bow-tie effect (Gomez-Landesa et al. 2004, Tan et al. 2006)
421 whereby observations further from nadir account for a larger land surface area than those
422 observations at nadir. Tan et al. (2006) also explain that the surface area contributing to a
423 MODIS observation is always larger than the grid cell because of the triangular point-
424 spread function. MODIS Level 3 products, such as the VCF, are multi-temporal
425 composites of the best Level 1B data available for a given location within a time interval.
426 Factors such as proximity to nadir and aerosol contamination contribute to the selection
427 of the data that will best describe ground features. Higher latitudes will have increasingly
428 more nadir and near-nadir pixels available for incorporation into a Level 3 data because
429 of the increasing degree of scan line overlap toward the poles, and more opportunities for
430 larger overlap between satellite observations and the grid cells into which they are
431 mapped (Robert Wolfe, personal communication).

432 Figure 9 shows a lake outline and one pixel's corners in northern Alaska (68.9N,
433 151.3W) overlaying both MODIS and Landsat TM from 6/14/2008 and Google Earth
434 basemap data. This example demonstrates that (1) MODIS Level 3 grid cells overlay the
435 correct earth features irrespective of the projection in which they are cast, (2) there is no
436 apparent geo-location degradation at high latitudes, and (3) features maintain their spatial

arrangement when displayed in Google Earth. The regular 10x10 dot grids, constrained by VCF grid cells, provide a way of estimating TCC in an area with which the boundaries are presumed to correspond. Each dot is used to represent an area that is 1/10 the area of a MODIS pixel. The 100 regularly arranged dots within the boundary of each site's corresponding pixel provide point-based estimates of areal values of TCC, while the pixels themselves are geo-located approximations of the actual land surface that provided the radiance values recorded by the satellite. This method, recommended by Hall et al. (2008), provides an intuitive and easily replicated means of performing pixel-level validation, and assessing sub-pixel variability, of MODIS Level 3 geophysical maps.

While our Quickbird TCC interpretations are not the definitive assessment of tree cover at the 396 sites, they represent our best estimates. We did not examine how the differences in acquisition time between the Quickbird and MODIS VCF imagery may have increased variability between the two estimation methods. However (1) the VCF is a temporal composite designed to minimize sensitivity to a specific time of year, (2) we gave preference to Quickbird imagery obtained from May to September when ground features aren't obscured by long shadows from low sun angles, and (3) the vast majority of sites were dominated by conifers whose crowns are visible regardless of season.

Cases where forest disturbance occurs between the acquisitions of each data source could contribute to variability of our ground reference with MODIS estimates. One case involves a forest disturbance at a validation site after the 2005 MODIS data and prior to a Quickbird acquisition used for ground reference. For example, a disturbance after the 2005 VCF dataset but prior to the acquisition of a Quickbird image used to select a site could affect forest cover that the VCF had already mapped. Depending on the nature of the disturbance, the ground reference and MODIS estimates could be based

461 on significantly different forest conditions. Our ground reference sites were chosen in
462 GE with Quickbird imagery where there were relatively homogenous forest conditions
463 and no visual signs of recent disturbances. This site selection method was a screening
464 process, decreasing the likelihood of validating mixed MODIS pixels and changed pixels.
465 A second case may occur if a site selected using a 2002 Quickbird acquisition
466 experienced a subsequent tree cover altering disturbance prior to the 2005 VCF. Such
467 cases will introduce noise into the relationship of the VCF to the ground reference
468 estimates. Regarding the likelihood of a burn at one of our validation sites, Hicke et al.
469 2003 indicate that 1% of the North American boreal forest biome may burn each year.
470 SPOT-VEGETATION estimates of boreal forest fire indicate that about 1% of the
471 circumpolar boreal burned from 2000-2004 (Bartalev et al. 2007). Similarly, Potapov et
472 al. (2008) estimated that approximately 1% of the area of forest cover loss in the boreal
473 biome was due to wildfire from 2001-2005, while forest cover loss as a percent of year
474 2000 forest area was 5.63% for North America.
475
476 **Discussion**
477 This validation helps establish the limits of the VCF for mapping the taiga-tundra
478 ecotone on a global scale. The accuracy and precision of global products such as the
479 VCF must be assessed to determine their utility for detecting subtle changes to the taiga-
480 tundra ecotone.
481 A comparison of VCF-to-VCF variability and interpreter-to-interpreter variability
482 provided an unexpected result. We note the following: (1) each inter-annual VCF percent
483 crown cover RMSE (9.5 – 10.8%) and RMSD value (6.8 – 7.8%) was smaller than the
484 image-interpreters' percent TCC RMSE (14.8%) and RMSD (18.7%) and (2) each inter-
485 annual VCF R^2 value (0.74 – 0.80) was higher than the interpreter R^2 (0.73). In the

majority of cases, slopes were not significantly different from 1 and intercepts were not significantly different from zero, however the results, specifically the RMSE and RMSD values, point out the difficulty of working in short-stature, open forests interspersed with shrubs of varying heights, both for image-interpreters and for analysts generating machine-processed standard products. In the ideal case of perfect, completely reproducible estimates of tree canopy cover from Quickbird, then we would expect the VCF-interpreter comparisons to have higher R^2 values and smaller RMSE and RMSD values. Interpreters were themselves quite variable, and that variability, which has no bearing on the quality of the VCF estimates, is manifested in the comparison.

Google Earth saved money and time by providing free high-resolution imagery across tens of thousands of kilometers of inhospitable, inaccessible terrain. However, the use of GE imagery comes at a cost. Some key factors that affected the interpretation of tree cover were the inability to manipulate or enhance Quickbird imagery in GE, the combination of view and high-latitude sun angle and the similar appearance of trees and shrubs. The Quickbird data's near-infrared channel is unavailable in GE, removing a potentially valuable tool for interpreting vegetation on screen. The GE imagery also lacks the ability to perform contrast enhancements. Additionally, in some instances the combination of the arrangement of forest patches and tree shadows with certain sun and view angles may have obscured tree cover, or led to false identification of tree cover. Regional differences in tree and shrub types and appearance may have, in some cases, affected tree cover estimates.

The VCF is a MODIS satellite map of a geophysical variable (tree canopy cover). The pixels of this map have attribute and geo-location information and are intended to be used along with other geographically referenced spatial data. Thus, the pixel locations

510 are presumed to represent those earth features with matching geo-location. It is for this
511 reason that pixel-level validation is useful, even with the variety of documented
512 uncertainties from the input satellite data, as it provides users, who will relate these pixels
513 to other spatial data, with a fundamental understanding of the accuracy of the product at
514 its finest resolution.
515
516 *Implications for Future Work: Mapping Tree Cover Changes at the Taiga-Tundra*
517 *Ecotone*
518 Callaghan et al. (2002a) reviewed the global importance of the taiga-tundra
519 boundary. They highlight the difficulties in understanding and representing the location
520 of this transition zone and in how to monitor its fluctuations. Although there are a number
521 of characteristics that aid delineation of this boundary, such as tree growth form, height,
522 age and aggregation, the distribution of trees is probably the most logical way of
523 presenting the regional transition from trees to tundra (Callaghan et al. 2002b). Rees et
524 al. (2002) discussed the importance of spatial resolution on the definition of treeline.
525 Stow et al. (2004) acknowledge the need for multi-scale mapping of vegetation
526 variability in the northern latitudes. Mapping the distribution of trees along the taiga-
527 tundra boundary in the circumpolar Arctic will be mostly at continental to global scales
528 but must also account for finer scale patterns that reveal gradual transitions. Examining
529 the heterogeneity of groups of 500m VCF pixels may help identify forest patches and
530 gaps (i.e., areas of similar tree distribution). Identifying landscape components formed
531 by groups of similar, adjacent pixels at a few scales establishes a foundation on which to
532 apply clear rules and definitions of ecotone location and extent. This process uses the
533 spatial context in which individual pixels exist (the values of surrounding pixels) to

534 reduce the data volume while advancing understanding of landscape patterns and
535 components. The performance of the VCF at the pixel level is important for
536 understanding the fundamental association of the predicted data with observed data. This
537 pixel-level approach assesses the VCF's utility for regional tree cover mapping in the
538 taiga-tundra transition zone. The patterns that these pixels reveal can help form the basis
539 of the dataset that can be observed and analyzed for change through time.

540 McMahon et al. (2004) discussed a robust basis for mapping ecological regions
541 and established a framework for both identifying and mapping ecoregions. This
542 framework involves identifying an extent, a grain/resolution, and a scale for the area
543 being examined and accounts for how the heterogeneity of conditions affects the
544 delineation of a boundary. The forest gaps and patches that form the spatial patterns of
545 the taiga-tundra ecotone represent internal heterogeneity that is difficult to capture on a
546 continental-global scale map. The continuous tree cover mapping provided by the VCF
547 product allows groups of pixels that represent patches and gaps to have attributes
548 representing internal variability that capture the gradual nature of the boundary. The
549 spatial variability, or texture, of the VCF product along with ancillary data may produce
550 maps that replicate forest cover variability in a way that discrete land cover classification
551 cannot, and may facilitate closer monitoring of subtle changes in the ecotone. In fact,
552 according to Hansen et al. (2002b), the VCF was developed because continuous classes
553 can represent the spatial heterogeneity better than fixed land cover classes, particularly in
554 land cover transition zones.

555 Given the inter-annual scatter noted between individual VCF observations, we
556 suggest that the taiga-tundra ecotone may be more reliably delineated and monitored over
557 time by considering groups of VCF observations rather than individual pixels. In this

558 scenario, any number of grouping algorithms – clustering processors, decision-tree
559 classifiers, image segmentations – could be used to identify VCF pixels with similar
560 canopy cover attributes. The mean and variance of the grouped pixels might then be used
561 to define a band of canopy cover conditions that represents the taiga-tundra transition
562 zone. Such an approach, one that groups adjacent pixels based on a defined level of
563 similarity, may mitigate spurious canopy cover error caused by VCF variability at the
564 pixel level.

565 To further improve the VCF product for work in northern regions, we provide the
566 following recommendations for subsequent iterations of the VCF products:

567 1. The addition of a water mask, which was available in the Collection 3
568 version, would be useful particularly for northern latitudes where low
569 tree cover and water bodies can be difficult to distinguish without
570 water-coded pixels.

571 2. Completion of the Collection 4 VCF tiles above 70° N would be
572 helpful for tracking changes at the northern edge of the taiga-tundra
573 transition zone, particularly in the lowlands just north of the Siberian
574 Trappes (Taimyr-Central Siberian tundra ecoregion) in Russia and at
575 the northern tip of Scandinavia (Scandinavian Montane Birch forest
576 and grasslands ecoregion) (UNEP/GRID-Arendal 2007).

577 3. Continued refinement of the VCF algorithm for low percent canopy
578 cover areas.

579

580 **Conclusion**

Accurate mapping of the taiga-tundra ecotone is important for monitoring subtle changes at the northern limits of the boreal forest. Documenting tree cover in this region using satellite-derived maps provides a means to continually assess changes in the transition between forest and tundra. The results of this study indicate the VCF's potential utility for the circumpolar taiga-tundra region and limitations inherent in its use, highlighted by its tendency to overestimate percent canopy cover in sparsely forested areas of the circumpolar taiga-tundra transition zone. This overestimation demonstrates to potential users of the VCF maps that this product may not be suitable for detailed mapping and monitoring of tree cover, particularly tree cover below 20%, at the product's finest (500m pixel) level of detail.

References

Bunn, A.G., & Goetz, S.J. (2006). Trends in satellite-observed circumpolar photosynthetic activity from 1982 to 2003: The influence of seasonality, cover type, and vegetation density. *Earth Interactions, 10*, 19.

Callaghan, T.V., Crawford, R.M.M., Eronen, M., Hofgaard, A., Payette, S., Rees, W.G., Skre, O., Sveinbjornsson, J., Vlassova, T.K., & Werkman, B.R. (2002a). The dynamics of the tundra-taiga boundary: An overview and suggested coordinated and integrated approach to research. *Ambio*, 3-5.

Callaghan, T.V., Werkman, B.R., & Crawford, R.M.M. (2002b). The tundra-taiga interface and its dynamics: Concepts and Applications. *Ambio,* 6-14.

Constantine, J.A., & Dunne, T. (2008). Meander cutoff and the controls on the production of oxbow lakes. *Geology, 36*, 23-26.

Crawford, R.M.M., Jeffree, C.E. & Rees, W.G. (2003). Paludification and forest retreat in northern oceanic environments. *Annals of Botany, 91*, 223-226. doi:10.1093/aob/mcfl85.

Cross, A.M., Settle, J.J., Drake, N.A. & Paivinen, R.T.M. (1991). Subpixel measurement of tropical forest cover using AVHRR data. *International Journal of Remote Sensing*, 12,1119-1129.

Curran, P.J. & Hay, A.M. (1986). The importance of measurement error for certain

procedures in remote sensing at optical wavelengths. *Photogrammetric Engineering and Remote Sensing*, *52*, 229–241.

Esper, J., & Schweingruber, F.H. (2004). Large-scale treeline changes recorded in Siberia. *Geophysical Research Letters, 31*, 1-5.

Frey, K. E., & Smith, L. C. (2007), How well do we know northern land cover? Comparison of four global vegetation and wetland products with a new ground-truth database for west Siberia. *Global Biogeochemical Cycles, 21*, GB1016. doi:10.1029/2006GB002706.

Goetz, S.J., Bunn, A.G., Friske, G.J., & Houghton, R.A. (2005). Satellite-observed photosynthetic trends across boreal North America associated with climate and fire disturbance. *Proceedings of the National Academy of Sciences U S A.,* 102,13521-13525.

Gomez-Landesa, E., Rango, A., & Bleiweiss, M. (2004). An algorithm to address the MODIS bowtie effect. *Canadian Journal of Remote Sensing, 30:*4, 644-650.

Hall, D.K., Box, J.E., Casey, K.A., Hook, S.J., Shuman, C.A., & Steffen, K. (2008). Comparison of satellite-derived and in-situ observations of ice and snow surface temperatures over Greenland. *Remote Sensing of Environment, 112,* 3739-3749.

Hansen, M.C., DeFries, R.S., Townshend, J.R.G., Marufu, L., & Sohlberg, R. (2002a). Development of a MODIS tree cover validation data set for Western Province, Zambia. *Remote Sensing of Environment, 83*, 320-335.

Hansen, M.C., DeFries, R.S., Townshend, J.R.G., Sohlberg, R., Dimiceli, C., & Carroll, M. (2002b). Towards an operational MODIS continuous field of percent tree cover algorithm: examples using AVHRR and MODIS data. *Remote Sensing of Environment, 83*, 303-319.

Hansen, M.C., Defries, R., Townshend, J., Carroll, M., Dimiceli, C. & Sohlberg, R. (2003). Global percent tree cover at a spatial resolution of 500 meters: first results of the MODIS vegetation continuous fields algorithm. *Earth Interactions*, *7,* 1-15.

Hassol, S.J. (2004). Arctic Climate Impact Assessment: Impacts of a Warming Arctic. Cambridge University Press, http://www.acia.uaf.edu (la=Aug. 27, 2008). 146 pgs.

Heiskanen, J. (2008). Evaluation of global land cover data sets over the taiga-tundra transition zone in northernmost Finland. *International Journal of Remote Sensing*, *29*:13, 3727-3751

Heiskanen, J., & Kivinen, S. (2008). Assessment of multispectral, -temporal and -angular MODIS data for tree cover mapping in the tundra–taiga transition zone. *Remote Sensing of Environment, 112*, 2367-2380.

664 IPCC. (2007). Climate Change 2007: The Physical Science Basis. Contribution of
665 Working Group I to the Fourth Assessment Report of the Intergovernmental Panel on
666 Climate Change [Solomon, S., D. Qin, M. Manning, Z. Chen, M. Marquis, K.B. Avery,
667 M. Tignor and H.L. Miller (eds.)]. Cambridge University Press, Cambridge, United
668 Kingdom and New York, NY, USA, 996 pp.
669
670 Kurz, W.A., Stinson, G., & Rampley, G. (2007). Could increased boreal forest ecosystem
671 productivity offset carbon losses from increased disturbances? *Philosophical*
672 *Transactions of the Royal Society B,* (doi:10.1098/rstb.2007.2198).
673
674 Kurz, W.A., Dymond, C.C., Stinson, G, Rampley, G.J., Neilson, E.T., Carroll, A.L.,
675 Ebata, T., & Safranyik, L. (2008a). Mountain pine beetle and forest carbon feedback to
676 climate change. *Nature, 452,* 987-990.
677
678 Kurz, W.A., Stinson, G., Rampley, G.J., Dymond, C.C., & Neilson, E.T. (2008b). Risk of
679 natural disturbances makes future contribution of Canada's forests to the global carbon
680 cycle highly uncertain. *Proceedings of the National Academy of Sciences U.S.A., 105,*
681 1551-1555.
682
683 Liu, L., & Mishchenko, M.I. (2008). Toward unified satellite climatology of aerosol
684 properties: Direct comparisons of advanced level 2 aerosol products. *Journal of*
685 *Quantitative Spectroscopy & Radiative Transfer, 109,* 2376-2385.
686
687 Luedeling, E., & Buerkert, A. (2008). Typology of oases in northern Oman based on
688 Landsat and SRTM imagery and geological survey data. *Remote Sensing of Environment,*
689 *112*, 1181-1195.
690
691 McMahon, G., Wiken, E.B., & Gauthier, D.A. (2004). Toward a scientifically rigorous
692 basis for developing mapped ecological regions. *Environmental Management, 34*, S111-
693 S124.
694
695 Mayaux, P., & Lambin, E.F. (1997). Tropical forest area measured from global land-
696 cover classifications: inverse calibration models based on spatial textures. *Remote*
697 *Sensing of Environment*, *59*, 29-43.
698
699 Morisette, J.T., Nickeson, J.E., Davis, P., Wang, Y., Tian, Y., Woodcock, C.E.,
700 Shabanov, N., Hansen, M., Cohen, W.B., Oetter, D.R., & Kennedy, R.E. (2003). High
701 spatial resolution satellite observations for validation of MODIS land products: IKONOS
702 observations acquired under the NASA Scientific Data Purchase. *Remote Sensing of*
703 *Environment, 88,* 100-110.
704
705 Myneni, R. B., Keeling, C. D., Tucker, C. J., Asrar, G. & Nemani, R. R. (1997).
706 Increased plant growth in the northern high latitudes from 1981 to 1991. *Nature, 386,*
707 698–702.
708
709 Pisek, J., & Chen, J.M. (2007). Comparison and validation of MODIS and
710 VEGETATION global LAI products over four BigFoot sites in North America. *Remote*
711 *Sensing of Environment, 109,* 81-94.

712
713 Potapov, P., Hansen, M.C., Stehman, S.V., Loveland, T.R., & Pittman, K. (2008).
714 Combining MODIS and Landsat imagery to estimate and map boreal forest cover loss.
715 *Remote Sensing of Environment, 112*, 3708-3719.
716
717 Randerson, J. T., Field, C. B., Fung, I. Y. & Tans, P. P. (1999). Increases in early season
718 ecosystem uptake explain recent changes in the seasonal cycle of atmospheric CO_2 at
719 high northern latitudes. *Geophysical Research Letters, 26*, 2765–2768.
720
721 Rees, G., Brown, I., Mikkola, K., Virtanen, T., & Werkman, B. (2002). How can the
722 dynamics of the tundra-taiga boundary be remotely monitored? *Ambio*, 56-62.
723
724 Salomonson, V.V., & Appel, I. (2006). Development of the Aqua MODIS NDSI
725 fractional snow cover algorithm and validation results. *IEEE Transactions on Geoscience*
726 *and Remote Sensing, 44(7),*1747-1756.
727
728 Schuur, E.A.G., Bockheim, J., Canadell, J.G., Euskirchen, E., Field, C.B., Goryachkin,
729 S.V., Hagemann, S., Kuhry, P., Lafleur, P.M., Lee, H., Mazhitova, G., Nelson,
730 F.E., Rinke, A., Romanovsky, V.E., Shiklomanov, N., Tarnocai, C., Venevsky, S., Vogel,
731 J.G., & Zimov, S.A. (2008). Vulnerability of permafrost carbon to climate change:
732 implications for the global carbon cycle. *Bioscience, 58*, 701-714.
733
734 Serreze, M.C., & Francis, J.A. (2006). The arctic amplification debate. *Climate Change,*
735 76, 241–264.
736
737 Soja, A. J., Tchebakova, N. M., French, N. H. F., Flannigan, M. D., Shugart, H. H.,
738 Stocks, B. J.,Sukhinin, A.I., Parfenova, E.I., Chapin III, F.S., & Stackhouse, Jr., P.W.
739 (2007). Climate-induced boreal forest change: Predictions versus current observations.
740 *Global and Planetary Change*, *56*, 274–296.
741
742 Solomon, S., Qin, D., Manning, M., Chen, Z., Marquis, M., Avery, K. B., Tignor, M. &
743 Miller, H. L., editors. (2007). Summary for Policymakers. *Climate Change 2007: The*
744 *Physical Science Basis. Contribution of Working Group 1 to the Fourth Assessment*
745 *Report of the Intergovernmental Panel on Climate Change*. Cambridge University Press,
746 Cambridge, United Kingdom.
747
748 Stow, D.A., Hope, A., McGuire, D., Verbyla, D., Gamon, J., Huemmrich, F., Houston,
749 S., Racine, C., Sturm, M., Tape, K., Hinzman, L., Yoshikawa, K., Tweedie, C., Noyle,
750 B., Silapaswan, C., Douglas, D., Griffith, B., Jia, G., Epstein, H., Walker, D., Daeschner,
751 S., Petersen, A., Zhou, L.M., & Myneni, R. (2004). Remote sensing of vegetation and
752 land-cover change in Arctic Tundra Ecosystems. *Remote Sensing of Environment, 89*,
753 281-308.
754
755 Sun, G., Ranson, K.J., Kharuk, V.I., & Kovacs, K. (2004). Changes in the taiga-tundra
756 boundary observed with Landsat. *International Geoscience and Remote Sensing*
757 *Symposium Proceedings. 2004 IEEE International* , *2*, 722-724.
758

759 Thenkabail, P.S., Biradar, C.M., Noojipady, P., Cai, X.L., Dheeravath, V., Li, Y.J.,
760 Velpuri, M., Gumma, M., & Pandey, S. (2007). Sub-pixel area calculation methods for
761 estimating irrigated areas. *Sensors, 7*, 2519-2538.
762
763 Timoney, K.P., Laroi, G.H., Zoltai, S.C., & Robinson, A.L. (1992). The high subarctic
764 forest-tundra of northwestern Canada: Position, width, and vegetation gradients in
765 relation to climate. *Arctic*, *45*,1–9.
766
767 Tottrup, C., Rasmussen, M. S., Eklundh, L., & Jönsson, P. (2007). Mapping fractional
768 forest cover across the highlands of mainland Southeast Asia using MODIS data and
769 regression tree modeling. *International Journal of Remote Sensing, 28,* 23-46.
770
771 UNEP/GRID-Arendal, 'Ecoregions prioritised for conservation, in the Arctic (WWF
772 Global 200)', *UNEP/GRID-Arendal Maps and Graphics Library*, 2007,
773 <http://maps.grida.no/go/graphic/ecoregions-prioritised-for-conservation-in-the-arctic-
774 wwf-global-200> [Accessed 15 January 2009]
775
776 White, M.A., Shaw, J.D., & Ramsey, R.D. (2005). Accuracy assessment of the vegetation
777 continuous field tree cover product using 3954 ground plots in the south-western USA.
778 *International Journal of Remote Sensing, 26*, 2699-2704.
779
780 Wolfe, R.E., Nishihama, M., Fleig, A.J., Kuyper, J.A., Roy, D.P., Storey, J.C., & Patt,
781 F.S. (2002). Achieving sub-pixel geolocation accuracy in support of MODIS land
782 science. *Remote Sensing of Environment, 83,* 31-4.
783
784 Zhou L., Kaufmann R. K., Tian Y., Myneni R. B., & Tucker C. J. (2003). Relation
785 between interannual variations in satellite measures of northern forest greenness and
786 climate between 1982 and 1999. *Journal of Geophysical Research 108(DI),* 4004,
787 doi:10.1029/2002JD002510.
788
789 Zhu, Z., & Evans, D. L. 1994. U.S. forest types and predicted percent forest cover from
790 AVHRR data. *Photogrammetric Engineering & Remote Sensing, 60*, 525–53.
791
792
793
794
795
796
797
798
799
800
801
802
803
804
805
806

807
808
809
810
811
812
813
814
815 **Figures & Tables**

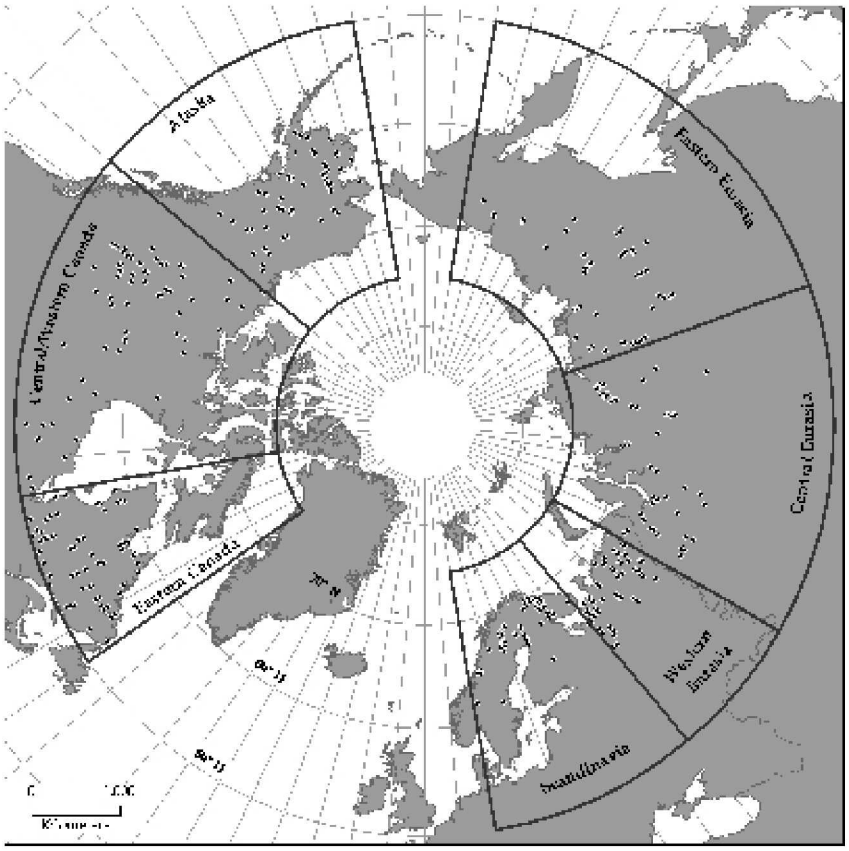

816

817 **Figure 1** Validation sites by zone in Eurasia and North America**.**
818

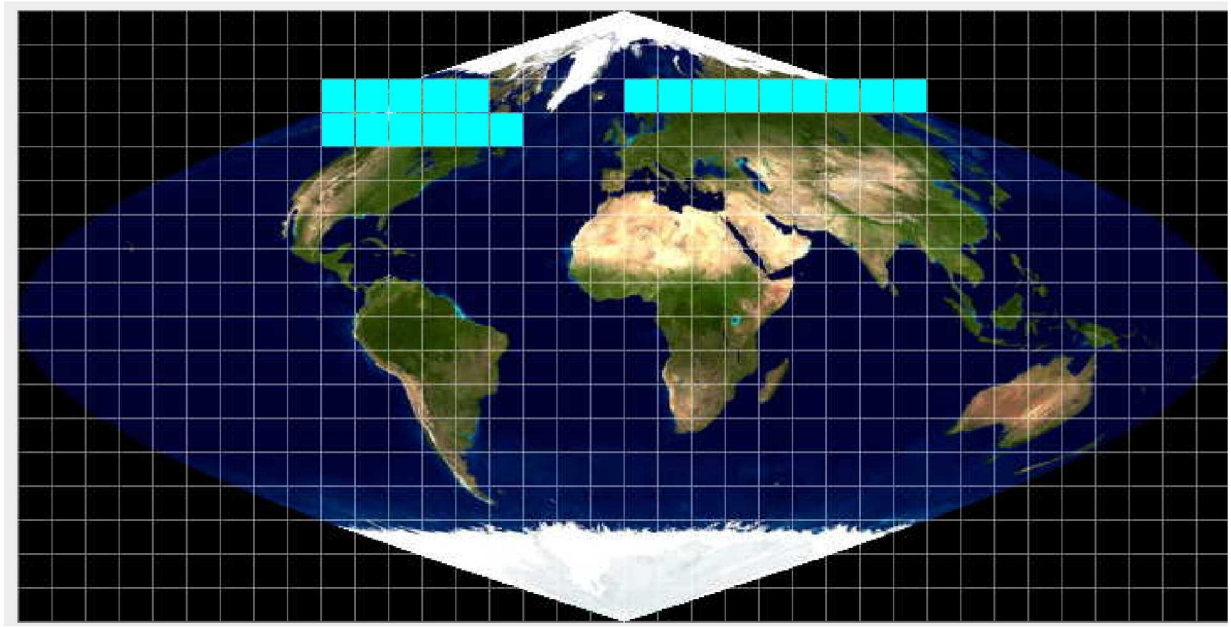

819

820 **Figure 2** Areas (in light blue) of MODIS tiles within which Quickbird imagery validation

821 sites were selected.

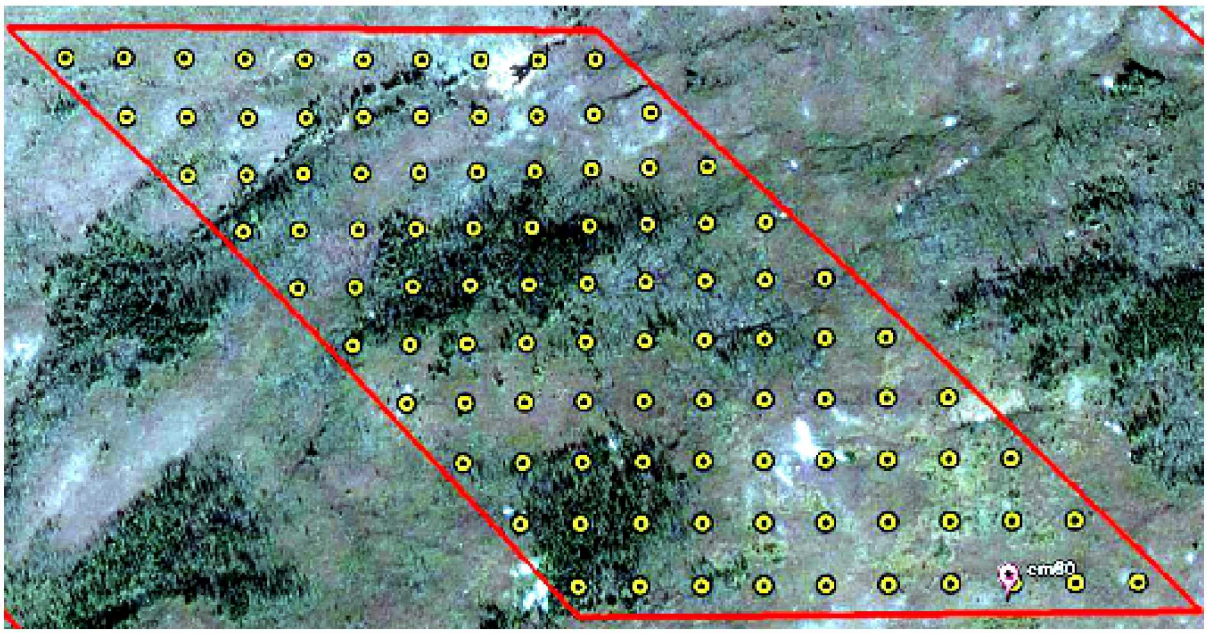

822

823 **Figure 3** An example of a VCF validation site in eastern Canada. The marker in the

824 lower right specifies the exact site selected using true-color Quickbird imagery in GE

825 with fixed enhancement. The red box represents the boundary of the corresponding VCF

826 pixel in the sinusoidal projection. The yellow dots mark the location of the 100 points

827 used to estimate %TCC. For this site, interpreters observed 23% TCC (i.e., 23 of 100

828 yellow dots fall on a tree crown) and the VCF estimated 25% canopy cover. Image

829 metadata was accessed through the "DigitalGlobe Coverage" layer in GE to provide
830 background information that in some cases aided interpretation of tree cover.

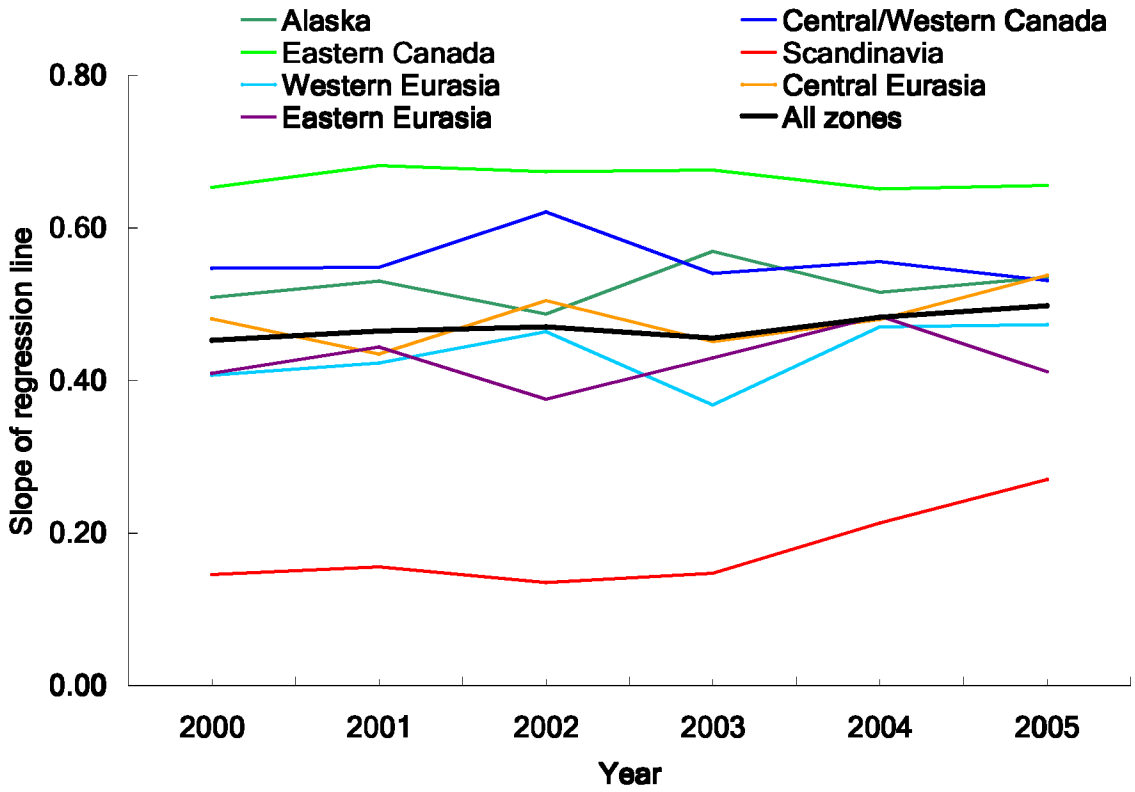

831

832 **Figure 4** Slopes of the regression line between VCF values and Quickbird estimates of
833 percent TCC for each year of the Collection 4 VCF data. The slopes for Scandinavia
834 may indicate a possible systematic bias in VCF processing for that area.

835

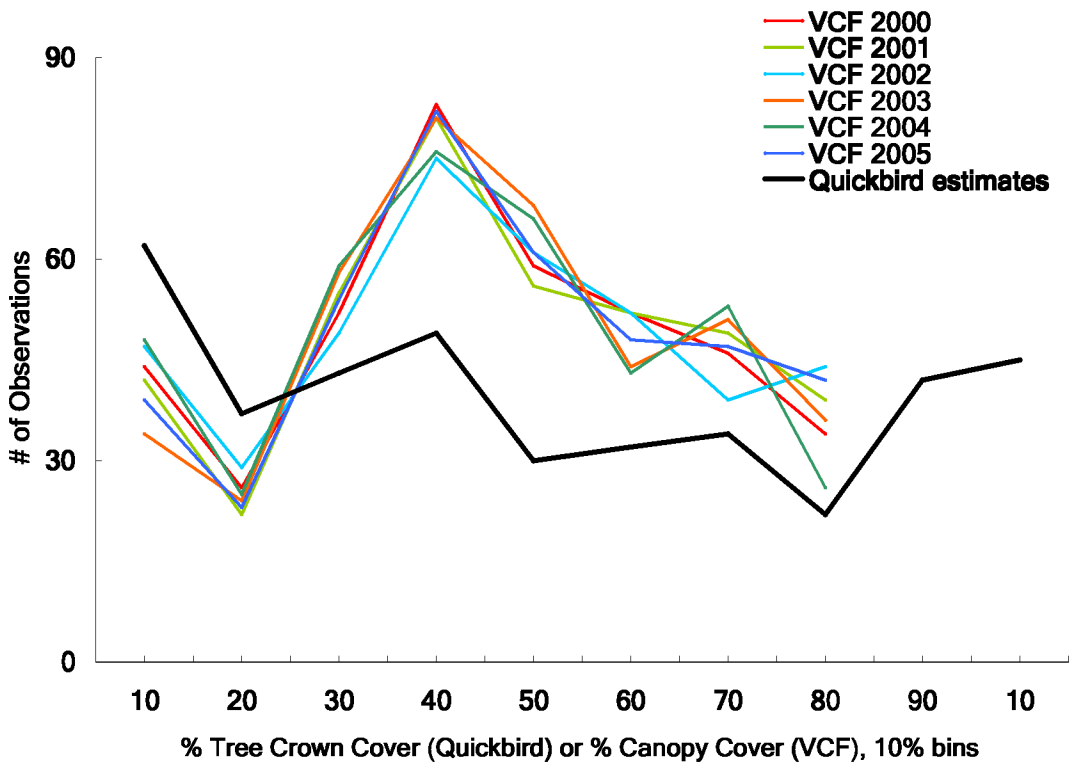

836
837 **Figure 5** Frequency distribution of percent TCC from Quickbird or percent canopy cover
838 from the VCF for 396 circumpolar boreal sites. The numbers along the X-axis denote the
839 bin maximum values. The Quickbird estimates report percent tree crown cover while the
840 VCF maps percent tree canopy cover.

841
842

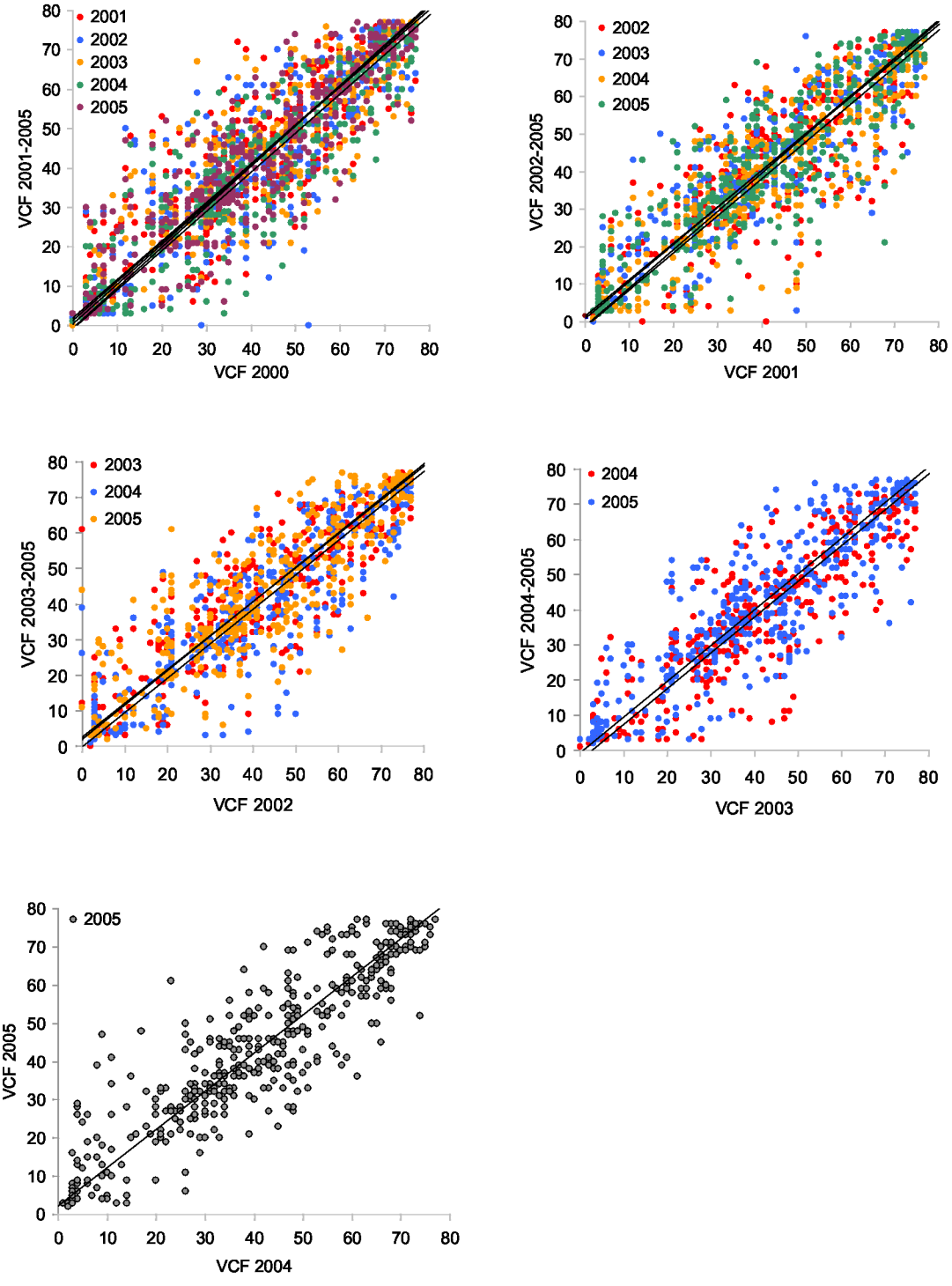

Figure 6 Plots of all VCF inter-annual combinations using RMA regression to demonstrate the variability inherent within the VCF. Each observation represents the value of each year's VCF data at a validation site (n = 403). For each plot, the earlier year is shown on the x-axis, with all subsequent years plotted on the y-axis.

Table 1 Summary of VCF RMA regression results showing Y-intercept (top row), slope (second row), RMSE and RMSD (third row), and R^2 values (bottom row) for all VCF inter-annual combinations (2000-2005) at 403 sites. P-values for tests of Y-intercept $\neq 0$ and slope $\neq 1$ are shown in italics adjacent to their corresponding regression coefficients. Significant differences shown in bold ($p<0.05$).

		2001		2002		2003		2004		2005	
2000	Y-intercept	0.42	*0.697*	-0.65	*0.566*	1.89	*0.082*	-0.93	*0.362*	1.27	*0.213*
	slope	1.01	*0.647*	1.03	*0.247*	0.98	*0.408*	1.00	*0.900*	1.00	*0.883*
	RMSE | RMSD	10.0	7.2	10.4	7.5	10.6	7.6	9.5	6.8	9.5	7.0
	R^2	0.78		0.77		0.76		0.80		0.80	
2001		--	--	-1.07	*0.248*	1.49	*0.159*	-1.34	*0.219*	0.86	*0.384*
		--	--	1.02	*0.454*	0.97	*0.181*	0.99	*0.566*	0.99	*0.549*
				10.2	7.3	9.9	7.0	10.2	7.3	10.2	7.3
				0.78		0.78		0.77		0.77	
2002		--	--	--	--	2.51	***0.015***	-0.30	*0.784*	1.90	*0.090*
		--	--	--	--	0.95	***0.035***	0.97	*0.192*	0.97	*0.200*
						10.0	7.1	10.4	7.5	10.8	7.8
						0.78		0.76		0.75	
2003		--	--	--	--	--	--	-2.85	***0.012***	-0.65	*0.587*
		--	--	--	--	--	--	1.02	*0.479*	1.02	*0.514*
								10.1	7.3	10.7	7.8
								0.77		0.74	
2004		--	--	--	--	--	--	--	--	2.20	***0.030***
		--	--	--	--	--	--	--	--	1.00	*0.982*
		--	--	--	--	--	--	--	--	9.6	7.0
		--	--	--	--	--	--	--	--	0.79	

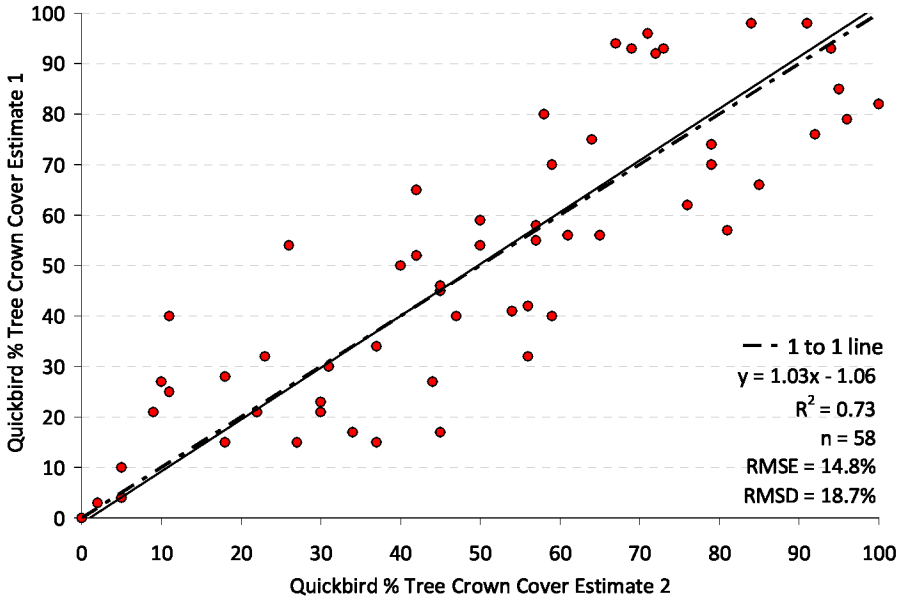

860

861 **Figure 7** RMA regression showing the relationship of replicated TCC interpretations

862 from Quickbird data by different interpreters for selected sites. The difference between

863 the Y-intercept and 0, and the slope and 1 are not significant ($p = 0.12$ and $p = 0.09$).

864
865
866

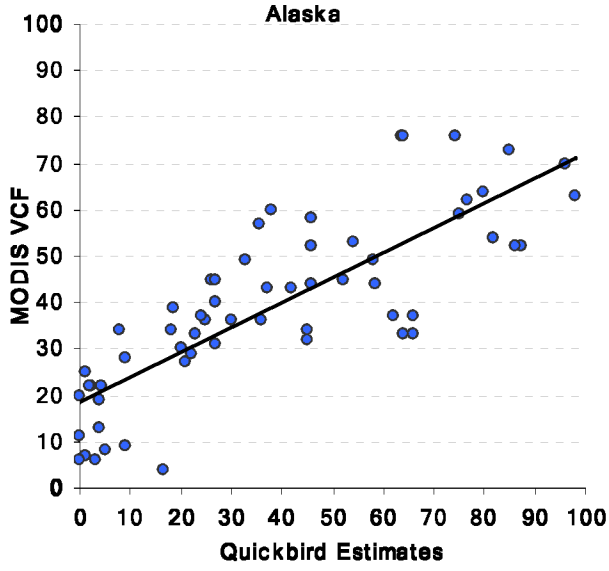
Alaska
MODIS VCF
Quickbird Estimates
0 10 20 30 40 50 60 70 80 90 100

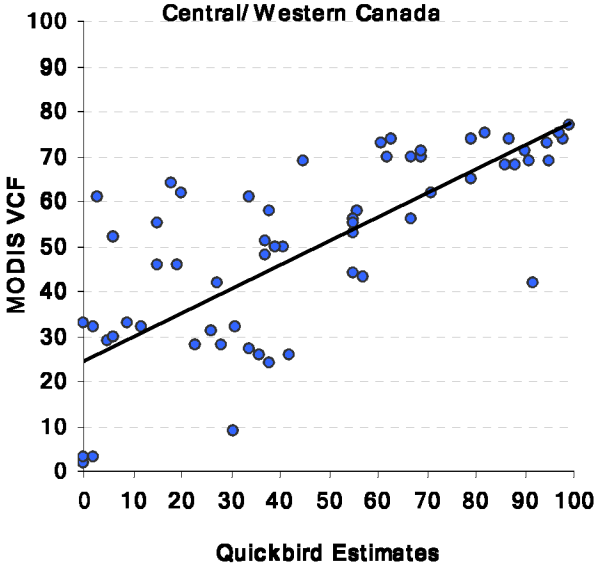
Central/ Western Canada
MODIS VCF
Quickbird Estimates
0 10 20 30 40 50 60 70 80 90 100

867

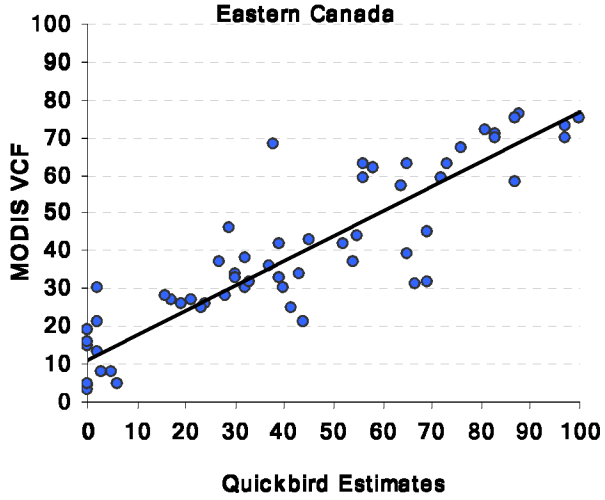
Eastern Canada
MODIS VCF
Quickbird Estimates
0 10 20 30 40 50 60 70 80 90 100

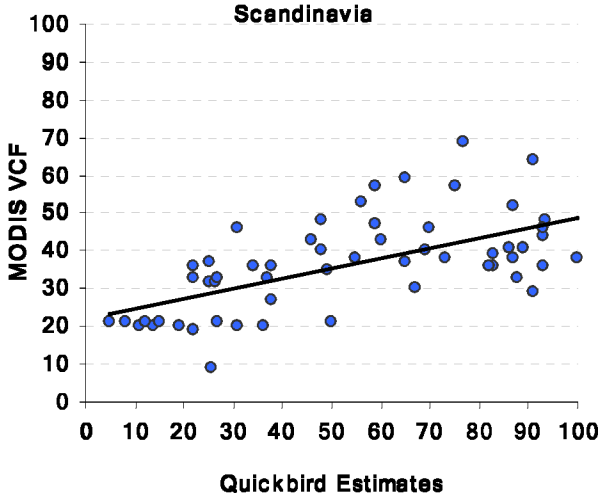
Scandinavia
MODIS VCF
Quickbird Estimates
0 10 20 30 40 50 60 70 80 90 100

868

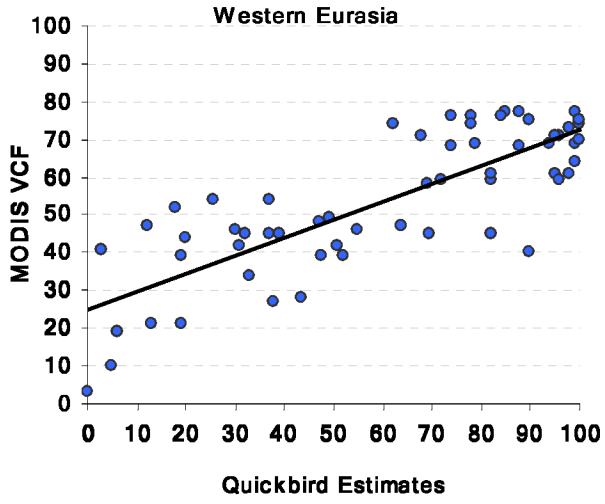
Western Eurasia
MODIS VCF
Quickbird Estimates
0 10 20 30 40 50 60 70 80 90 100

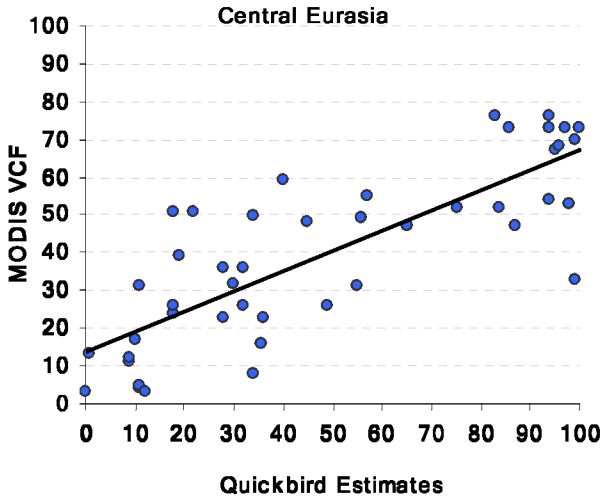
Central Eurasia
MODIS VCF
Quickbird Estimates
0 10 20 30 40 50 60 70 80 90 100

869

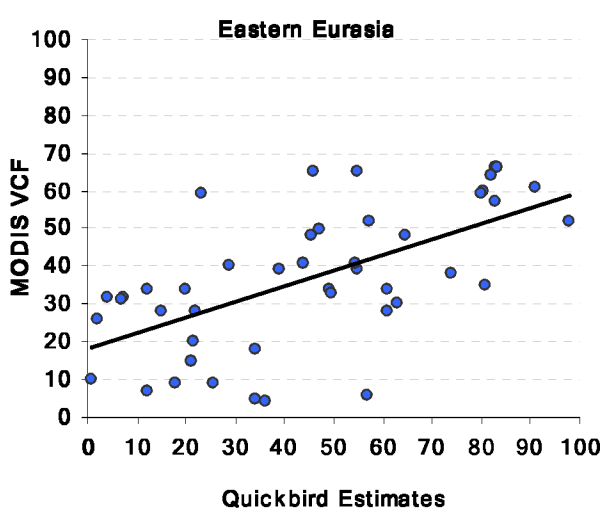

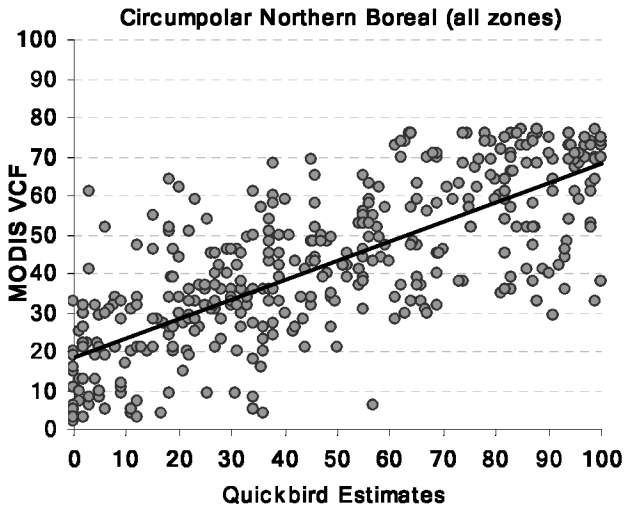

870

871 **Figure 8** Simple linear regression showing the relationship of MODIS 2005 VCF percent
872 canopy cover values with estimated percent TCC values from Quickbird imagery.

873

874 **Table 2** Summary of simple linear regression values representing the relationship of the
875 2005 VCF with the observed % TCC values from Quickbird data for each region and all
876 combined regions.

2005 VCF	R^2	RMSE	RMSD	Slope	P-value for slope ≠ 1	Y-intercept	P-value for Y-intercept ≠ 0	n
Alaska	0.66	10.9	17.2	0.54	< 0.001	18.6	< 0.001	60
Central/Western Canada	0.57	14.5	21.1	0.53	< 0.001	24.58	< 0.001	64
Eastern Canada	0.82	9.5	14.4	0.66	< 0.001	10.96	< 0.001	64
Scandinavia	0.38	9.7	28.6	0.27	< 0.001	21.83	< 0.001	58
Western Eurasia	0.65	10.9	21.0	0.47	< 0.001	24.91	< 0.001	59
Central Eurasia	0.66	13.2	22.4	0.54	< 0.001	13.51	< 0.001	45
Eastern Eurasia	0.38	14.4	22.9	0.41	< 0.001	18.37	< 0.001	46
All zones	0.57	13.4	21.3	0.5	< 0.001	18.36	< 0.001	396

877
878
879
880

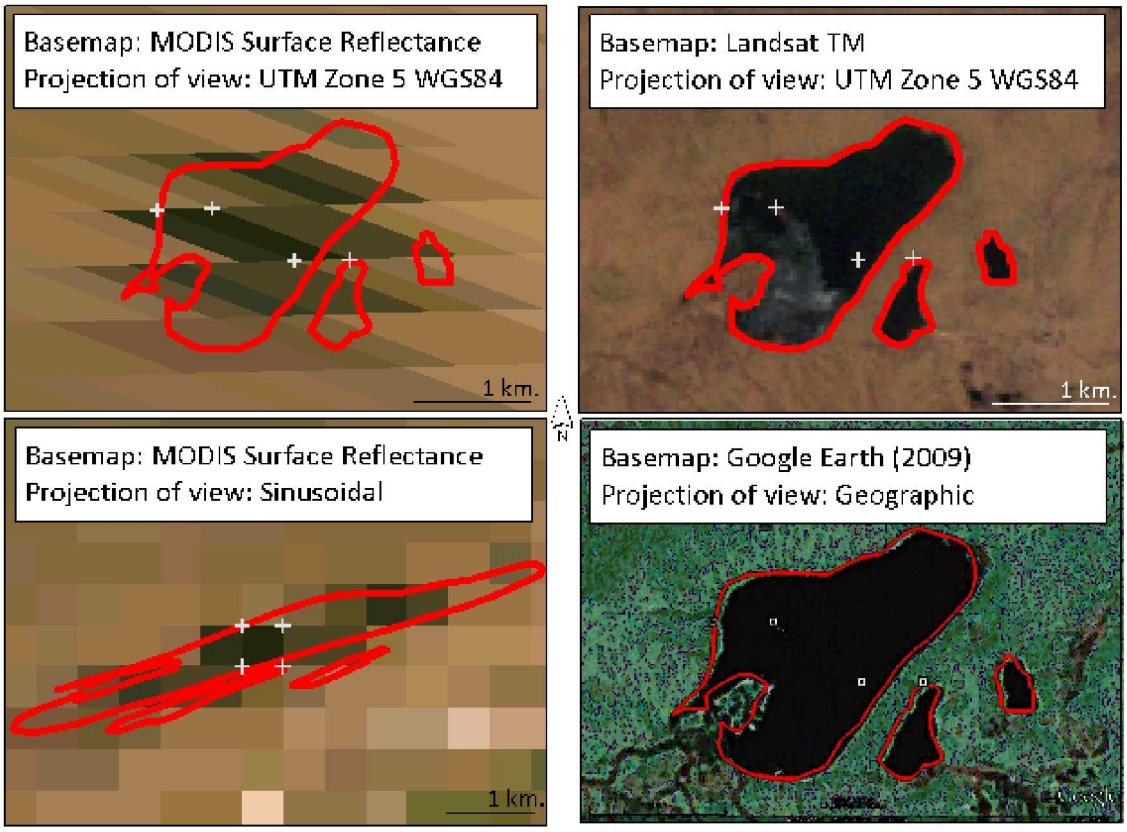

881
882 **Figure 9** An example of a feature (a lake) denoted by the red polygon, shown in MODIS
883 Level 3 data and Landsat TM data for 6/14/2008 and in Google Earth. The MODIS (in
884 the sinusoidal grid) is shown in both Landsat TM's UTM projection and MODIS's
885 sinusoidal projection. The 4 corners of the lake's center pixel are show in each image as
886 reference, to show that the geo-location of the pixel with respect to the lake polygon does
887 not change regardless of view projection.